Article

Separation of CO and N by Adsorption in C Schwarzite: A Combination of Quantum Mechanics and Molecular Simulation Study

Jianwen Jiang, and Stanley I. Sandler

J. Am. Chem. Soc., **2005**, 127 (34), 11989-11997• DOI: 10.1021/ja0424575 • Publication Date (Web): 10 August 2005

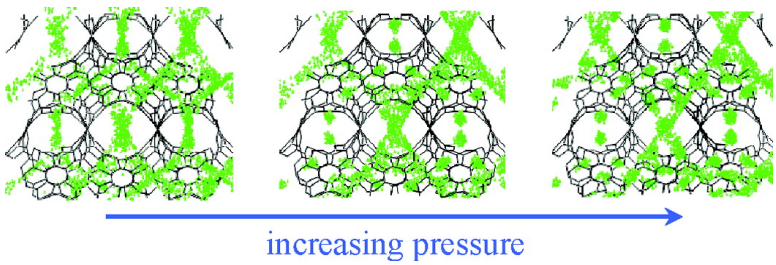

More About This Article

J|A|C|S
ARTICLES
Published on Web 08/10/2005

Separation of CO_2 and N_2 by Adsorption in C_{168} Schwarzite: A Combination of Quantum Mechanics and Molecular Simulation Study

Jianwen Jiang* and Stanley I. Sandler*

Contribution from the Center for Molecular and Engineering Thermodynamics, Department of Chemical Engineering, University of Delaware, Newark, Delaware, 19716

Received December 15, 2004; E-mail: jiangj@che.udel.edu; sandler@che.udel.edu

Abstract: Using a hierarchical multiscale approach combining quantum mechanics and molecular simulation, we have investigated the adsorption of pure CO_2 and N_2 and their mixture at room temperature in C_{168} schwarzite, as a model for nanoporous carbons. First, the adsorbate−adsorbent interaction potential is determined using ab initio quantum mechanics computations, and then the adsorption is predicted using full atomistic Monte Carlo simulations. The extents of adsorption, adsorption energies, and isosteric heats of pure CO_2 and N_2 simulated with the ab initio potential are found to be higher than those with the empirical Steele potential that had been developed from gas adsorption on planar graphite. The inclusion of the electric quadrupole moment of adsorbate in simulation has no discernible effect on N_2 adsorption but results in a larger extent of CO_2 adsorption at high coverages. The selectivity of CO_2 over N_2 in the C_{168} schwarzite from a model flue gas is predicted to be significantly larger with the ab initio potential than with the Steele potential. This illustrates the importance of an accurate adsorbate−adsorbent interaction potential in determining gas adsorption and suggests that nanoporous carbons might be useful for the separation of flue gases. As a comparison, the adsorption and selectivity of CO_2 and N_2 in ZSM-5 zeolites are also simulated with the experimentally validated potential parameters. The selectivity in the C_{168} schwarzite predicted with the ab initio or Steele potential is found to be larger than the selectivity in all-silica ZSM-5, but less than that in Na-exchanged ZSM-5 zeolites.

I. Introduction

Since the beginning of the industrial age, the atmospheric CO_2 concentration has increased from 280 to 380 parts per million (ppm). It has been suggested that this may have caused the recorded average global surface temperature rise of 0.6 °C over the past century.[1] The increased CO_2 is largely due to the vast amounts of the flue gases emitted by industrial and utility power generation plants using carbon-based fossil fuels. Flue gases are generally at or slightly above atmospheric pressure. Typically, the major components are N_2 and CO_2. They may also contain O_2, and trace contaminants such as NO_x, SO_x, etc. The compositions vary widely, depending on fuel composition, combustion system, and operating condition. Sequestration of the greenhouse gas CO_2 has been one of the most pressing issues in environmental protection. Prior to the sequestration or conversion, CO_2 must be captured and separated from other components in the flue gases. This is a big challenge in the process of CO_2 sequestration.[2]

Adsorption with alkanolamines was generally used for removal of CO_2 in natural gas treating.[3] However, membrane adsorption has the possibility of being a cost-effective and technically feasible technology for the separation of CO_2 from gas mixtures. For example, uncapped multiwalled carbon nanotube membranes have been found to be effective in the separation of CO_2 and N_2 from flue gases. At elevated temperatures and pressures, significant uptake of CO_2 was obtained, about 2 orders of magnitude greater than that of N_2.[4] Capillary-type facilitated transport membranes using amines as carriers or adsorbents have been used for the simultaneous separation and enrichment of CO_2 from model flue gases consisting of CO_2 and N_2.[5] ZSM-5 zeolite membranes have been prepared and tested for the separation of CO_2/N_2 mixtures, and CO_2 was found to be preferentially adsorbed.[6] Some other types of zeolites such as mordenite, faujasite, and chabazite, have also been used for the separation of CO_2/N_2 mixtures.[7]

Nanoporous carbon (NPC) membranes synthesized by the ultrasonic deposition of poly(furfuryl alcohol) on porous stainless steel have been found to result in very different permeation rates for gases with similar molecular dimensions.[8−10] For example, the permeance of O_2 is 2−30 times larger than that

(1) Service, R. F. *Science* **2004**, *305*, 962.
(2) Noble, R. D.; Agrawal, R. *Ind. Eng. Chem. Res.* **2005**, *44*, 2887.
(3) Kohl, A.; Nielsen, R. *Gas Purification*, 5th ed.; Gulf Publishing: Houston, TX, 1997.
(4) Andrews, R.; Jagtoyen, M.; Grulke, E.; Lee, K. H.; Mao, Z. A.; Sinnott, S. B. "Separation of CO_2 and N_2 from Flue Gases by Multi-Walled Carbon Nanotube Membranes"; Sixth Applied Diamond Conference/Second Frontier Carbon Technology Joint Conference, 2001, Auburn, AL.
(5) Teramoto, M.; Kitada, S.; Ohnishi, N.; Matsuyama, H.; Masumiya, N. *J. Membr. Sci.* **2004**, *234*, 83.
(6) Bernal, M. P.; Coronas, J.; Menendez, M.; Santamaria, J. *AIChE J.* **2004**, *50*, 127.
(7) Table 6 in Bernal, M. P.; Coronas, J.; Menendez, M.; Santamaria, J. *AIChE J.* **2004**, *50*, 127.
(8) Shiflett, M. B.; Foley, H. C. *Science* **1999**, *285*, 1902.

Table 1. Site−Site Potential Parameters[a]

	N_2	CO_2		ab initio potential			Steele potential		
	N–**N**	**C**O_2–**C**O_2	**C**O_2–**C**O_2	**C**–**N**	**C**–**C**O_2	**C**–**C**O_2	**C**–**N**	**C**–**C**O_2	**C**–**C**O_2
σ (Å)	3.32	2.785	3.064	3.542	3.443	3.132	3.36	3.11	3.16
ϵ/k_B (K)	36.4	28.999	82.997	36.902	35.921	55.180	33.4	27.0	45.6
q (e)	−0.482	+0.6645	−0.33225						

[a] The bold atoms are interaction sites, and the underlined atoms are on the adsorbent surface.

of N_2 depending on the NPC synthesis conditions. We envision that the NPC membranes may also lead to the efficient separation between CO_2 and N_2 in flue gases, which is the objective of this work.

In our previous studies,[11,12] in order to elucidate the adsorption behavior of O_2 and N_2 in a NPC membrane, the hypothetical C_{168} schwarzite was used as an adsorbent model to represent the amorphous NPC, and its interactions with O_2 and N_2 were modeled using the Steele potential[13,14] derived from the adsorption of O_2 and N_2 on planar graphite at zero coverage. With this empirical potential, the extents of adsorption of pure O_2 and N_2 in the C_{168} schwarzite were predicted from molecular simulations to be very close to each other and the adsorption selectivity (separation factor) between the two gases from a binary mixture was small. Therefore, the predicted adsorption behavior did not provide an explanation of the large difference in permeation rates between O_2 and N_2 found in experiment.[11,12] The use of the empirical Steele potential based on graphite for the interaction between a gas and the C_{168} schwarzite is an approximation that may not be accurate as the C_{168} schwarzite and graphite have different bonding and ring structures. The C_{168} schwarzite has convex and concave surfaces as a result of the combination of the aromatic sp^2 and aliphatic sp^3 hybridization of the carbon atoms and contains primarily six-member rings but also nonaromatic five-, seven-, and eight-membered rings. In contrast, graphite has a planar surface resulting from the pure sp^2 hybridization and only contains aromatic six-membered rings. As a consequence, the gas-carbon interaction potential might be influenced by the surface curvature and ring structure, which could change the localization of the electron density. In fact, the curvature-induced charge redistribution and polarization in curved carbon nanotubes have been recognized,[15] and the force field parameters of the gas-carbon interaction potential in carbon nanotubes have been found to be strongly curvature dependent.[16]

By accounting for the important effects of the surface curvature and ring structure, an accurate ab initio potential has been developed by us for the interaction of N_2 and O_2 with the C_{168} schwarzite from the first-principles quantum mechanics computations, which was then used in molecular simulations to predict the adsorption behavior.[17,18] This hierarchical multiscale approach has also been used by us in the modeling of N_2 adsorption on the surface of, and within, a buckyball C_{60} crystal.[19] With the ab initio potential, a large adsorptive separation was predicted between O_2 and N_2 in the C_{168} schwarzite, with N_2 adsorbing much more than O_2. That N_2 is adsorbed more strongly suggested, based on the arguments used to explain chromatographic separations, that O_2 will have a higher permeability through the schwarzite as have been observed in experiment. Those results reveal the importance of the interaction potential in determining correct adsorption behavior. Furthermore, the results with the ab initio potential imply that NPC adsorbents, such as the C_{168} schwarzite, can be useful for O_2 and N_2 separations.

In this work, we investigate the adsorption of pure CO_2 and N_2 and their binary mixture in the C_{168} schwarzite to examine the use of NPC membranes to separate CO_2 and N_2 in flue gases. Similar to our previous studies,[17,18] first we obtain the ab initio potential for the interaction of adsorbate−adsorbent from quantum mechanics (QM) computations and then predict the adsorption behavior from full atomistic Monte Carlo (MC) simulations.

In section II we briefly describe the atomic model for the adsorption system and the ab initio potential obtained in this work, followed in section III by a discussion of the simulation method, which includes grand canonical Monte Carlo simulation to predict the adsorption of both pure and mixed gases and canonical Monte Carlo simulation to evaluate the limiting adsorption properties. The results of the adsorption isotherm, adsorption energy, heat of adsorption, and the center-of-mass density distribution within the adsorbent calculated with both the ab initio potential and the Steele potential are presented and compared in section IV. Finally, conclusions are presented in section V.

II. Model and Potential

In our previous studies,[11,12,18,19] the adsorbate N_2 was represented as a two-site rigid molecule with a bond length of 1.10 Å. The intermolecular interaction was modeled by the isotropic pairwise additive site−site Lennard−Jones (LJ) potential

$$u_{ij}(r) = \sum_{\substack{\alpha\in i \\ \beta\in j}} \left\{ 4\epsilon_{\alpha\beta} \left[\left(\frac{\sigma_{\alpha\beta}}{r_{\alpha\beta}}\right)^{12} - \left(\frac{\sigma_{\alpha\beta}}{r_{\alpha\beta}}\right)^{6} \right] \right\} \qquad (1)$$

where α or β is the site in molecule i or j. The LJ potential parameters for the well depth $\epsilon_{\alpha\beta}$ and collision diameter $\sigma_{\alpha\beta}$ are given in Table 1, which, supplemented by an adjustable point quadrupole moment, were fitted by Murthy et al.[20] to a wide variety of the experimental bulk N_2 properties. Previously, for

(9) Shiflett, M. B.; Pedrick, J. F.; McLean, S. R.; Subramoney, S.; Foley, H. C. *Adv. Mater.* **2000**, *12*, 21.
(10) Strano, M. S.; Foley, H. C. *Carbon* **2002**, *40*, 1029.
(11) Jiang, J. W.; Klauda, J. B.; Sandler, S. I. *Langmuir* **2003**, *19*, 3512.
(12) Jiang, J. W.; Sandler, S. I. *Langmuir* **2003**, *19*, 5936.
(13) Bojan, M. J.; Steele, W. A. *Langmuir* **1987**, *3*, 116.
(14) Bojan, M. J.; Steele, W. A. *Langmuir* **1987**, *3*, 1123.
(15) Dumitrica, T.; Landis, C. M.; Yakobson, B. I. *Chem. Phys. Lett.* **2002**, *360*, 182.
(16) Kostov, M. K.; Cheng, H.; Cooper, A. C.; Pez, G. P. *Phys. Rev. Lett.* **2002**, *89*, 146105.
(17) Klauda, J. B.; Jiang, J. W.; Sandler, S. I. *J. Phys. Chem. B* **2004**, *108*, 9842.
(18) Jiang, J. W.; Klauda, J. B.; Sandler, S. I. *J. Phys. Chem. B* **2004**, *108*, 9852.
(19) Jiang, J. W.; Klauda, J. B.; Sandler, S. I. *J. Phys. Chem. B* **2005**, *109*, 4731.

simplicity, we did not consider the quadrupole moment of the N_2 molecule. However, as we shall see, the inclusion of the quadrupole moment makes negligible contribution to N_2 adsorption in the C_{168} schwarzite.

In this work, the quadrupole moment of N_2 is included, but rather than a point quadrupole moment or a complete charge distribution, a partial-charge model is used.[21] The N_2 molecule is assigned a negative charge q_N on each N atom, and a positive charge $-2q_N$ at its center-of-mass to maintain electroneutrality. The N_2-N_2 intermolecular interaction is then modeled as a combination of the site−site LJ and Coulombic potentials

$$u_{ij}(r) = \sum_{\substack{\alpha\in i \\ \beta\in j}} \left\{ 4\epsilon_{\alpha\beta}\left[\left(\frac{\sigma_{\alpha\beta}}{r_{\alpha\beta}}\right)^{12} - \left(\frac{\sigma_{\alpha\beta}}{r_{\alpha\beta}}\right)^{6}\right] + \frac{q_\alpha q_\beta}{4\pi\epsilon_0 r_{\alpha\beta}} \right\} \quad (2)$$

where $\epsilon_0 = 8.8542 \times 10^{-12}$ C^2 N^{-1} m^{-2} is the permittivity of vacuum. The LJ potential parameters $\epsilon_{\alpha\beta}$ and $\sigma_{\alpha\beta}$ are identical to those in eq 1 fitted by Murthy et al.[20] The partial charge of $q_N = -0.482e$ ($e = 1.6022 \times 10^{-19}$ C is the elementary charge) is used to reproduce the measured N_2 gas-phase quadrupole moment $Q_{N_2} = -4.67 \times 10^{-40}$(C·$m^2$) $= -1.4$ B.[22]

The adsorbate CO_2 is represented as a three-site molecule with a partial charge on each atom. The partial charge on C atom $q_C = +0.6645e$ is used to reproduce the measured CO_2 gas-phase quadrupole moment $Q_{CO_2} = -1.43 \times 10^{-39}$ (C·m^2) $= -4.3$ B;[22] due to electroneutrality the partial charge on O atom is $-0.5q_C$. The C−O bond is assumed to be rigid, and the bond length is 1.161 Å. The ∠OCO bond is flexible and governed by a harmonic potential $^1/_2 k_\theta(\theta - \theta_0)^2$ with the force constant $k_\theta/k_B = 153\,355.79$ (K/rad^2) and the equilibrium angle $\theta_0 = 180°$. The CO_2-CO_2 intermolecular interaction is also modeled using eq 2 with potential parameters given in Table 1, which were fitted by Harris and Yung to the experimental VLE data of bulk CO_2.[23] The Lorentz−Berthelot combining rules are used to calculate the LJ cross interaction parameters.

Adsorbent NPC membranes are amorphous and do not have well-defined structures, and consequently, the hypothetical C_{168} schwarzite[24] is used in this work to represent the NPC, as in our previous studies.[11,12,17,18] The C_{168} schwarzite has a simple periodic structure, with well-defined pores and channels, and carbon-surface curvatures similar to an NPC. In addition to the primary six-membered rings, there are also five-, seven-, and eight-membered rings. The unit cell of the C_{168} schwarzite has a length of 21.8 Å and 672 carbon atoms. There are two types of pores in the C_{168} schwarzite with average diameters of approximately 7 and 9 Å. The pores in the same layer are isolated from each other, but they are connected with those in the neighboring layers by channel intersections. The C−C bonds are assumed to be rigid, and the locations of the C atoms are frozen during the simulation. These assumptions should not significantly affect adsorption but may influence transport properties (which are not considered here).

The Steele potential derived from the experimental data of gas adsorption on planar graphite is often used to model gas adsorption on carbon-based surfaces.[25] However, as we have mentioned above, the empirical Steele potential may not be accurate for the C_{168} schwarzite, which has the nonzero curvature and nonaromatic rings. Consequently, we first calculate the interaction energies between a gas molecule and the C_{168} schwarzite from the ab initio QM computations, and then these interaction energies are fitted to an analytical potential. In our previous work, the ab initio potential for N_2 and O_2 with the C_{168} schwarzite has been developed.[17] The same method is used in this work to develop the ab initio potential for CO_2 interacting with the C_{168} schwarzite, and a brief description is given below.

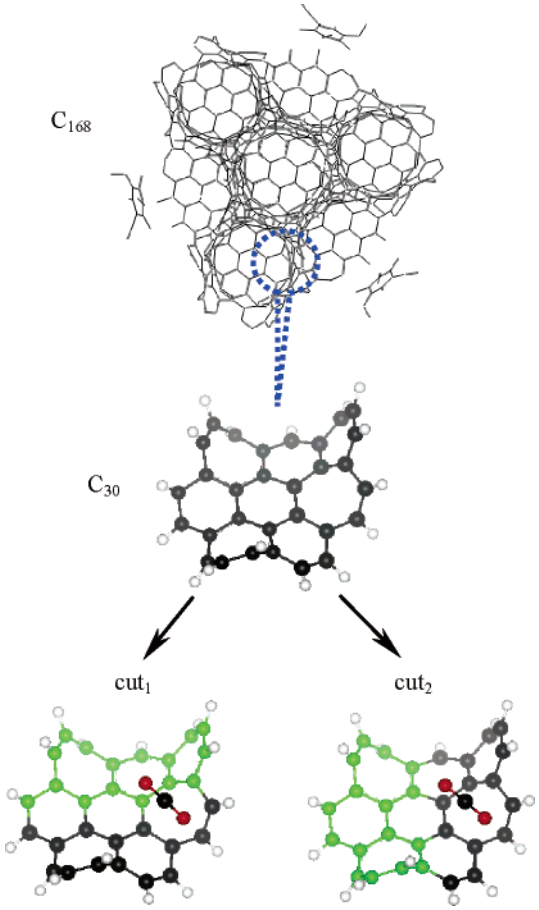

Figure 1. A cluster with 30 C atoms (C_{30}) used to represent the C_{168} schwarzite and the C_{30} cluster cut into two smaller segments in two ways cut_1 and cut_2. See text for details.

The interaction between a simple gas and the carbon surface is mainly of the van der Waals type; as a consequence, a high level QM method, e.g., CCSD(T) is required to accurately compute the weak interaction.[17] However, the computationally intensive CCSD(T) method is currently only possible for small systems and cannot be used for the large CO_2-C_{168} system of interest here. Instead, the interactions of CO_2 with a cluster model of the carbon surface were computed; similar to the development of the ab initio potential for gas−H_2O interaction in gas hydrates, in which only a cluster of molecules from the H_2O cage was used.[26] As illustrated in Figure 1, a cluster of 30 C atoms (C_{30}) cut from the channel intersection of the C_{168} was assumed to represent the C_{168}, and the cleaved C−C bonds in the C_{30} cluster were terminated with H atoms to maintain the

(20) Murthy, C. S.; Sing, K.; Klein, M. L.; McDonald, I. R. *Molecular Physics* **1980**, *41*, 1387.
(21) Talbot, J.; Tildesley, D. J.; Steele, W. A. *Faraday Discuss. Chem. Soc.* **1985**, *80*, 91.
(22) Buckingham, A. D.; Disch, R. L.; Dunmur, D. A. *J. Am. Chem. Soc.* **1968**, *90*, 3104.
(23) Harris, J. G.; Yung, K. H. *J. Phys. Chem.* **1995**, *99*, 12021.
(24) Vanderbilt, D.; Tersoff, J. *Phys. Rev. Lett.* **1992**, *68*, 511.
(25) Steele, W. *Appl. Surf. Sci.* **2002**, *196*, 3.
(26) Klauda, J. B.; Sandler, S. I. *J. Phys. Chem. B* **2002**, *106*, 5722.

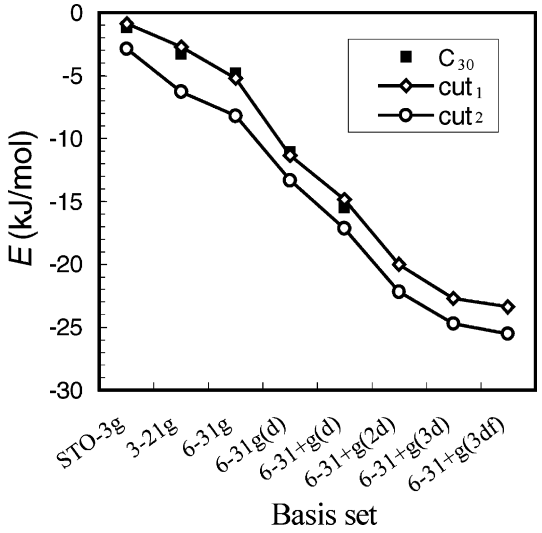

Figure 2. Basis set variation of the interaction energies computed using the MP2 method. The filled squares are the interaction energies of CO_2 with the whole C_{30} cluster, the unfilled diamonds are the sum of the interaction energies of CO_2 with the two segments from cut_1, and the unfilled circles are the sum of the interaction energies of CO_2 with the two segments from cut_2. The interaction energies at various basis sets from cut_1 were found to be in good agreement with those using the whole C_{30} cluster.

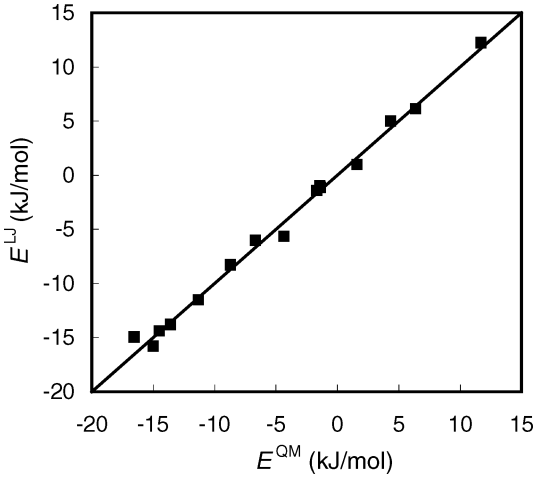

Figure 3. Interaction energies computed from QM versus those from the fitted LJ potential. The average absolute deviation for the 14 points is 0.545 kJ/mol.

original hybridization. But even so, the computation for the interaction of $C_{30}-CO_2$ is extremely time-consuming using the CCSD(T) method with a sufficiently large basis set. To accelerate the computation, the C_{30} cluster was further cut into two smaller segments, and the interactions of CO_2 with these segments were computed. To determine which way to cut the C_{30} cluster to obtain accurate interaction energies while using only a portion of the C_{30} cluster, the interactions with CO_2 before and after a trial cut were computed and compared using a computationally efficient, but lower level, MP2 method. Figure 1 illustrates two different cuts of the C_{30} cluster into two segments (one with 14 C atoms and the other with 16 C atoms) referred to as cut_1 and cut_2, in which CO_2 was at the energy minimum position in the C_{168} channel intersection estimated from a Monte Carlo simulation. In each, the cleaved C−C bonds were also terminated with H atoms, and the interaction energies with CO_2 were then computed and summed for both segments. Shown in Figure 2 are the interaction energies from cut_1, cut_2, and the whole C_{30} cluster computed with the MP2 method and various basis sets. Good agreement between cut_1 and the whole C_{30} cluster was obtained, and therefore the two smaller segments from cut_1 were used to compute the interaction energies with CO_2 at various separation distances and orientations.

We have shown previously[27] that the effect of an increase in basis set size on the interaction energy is nearly independent of the level of electron correlation; that is, at any basis set, the interaction energies of the CCSD(T) and MP2 are shifted essentially only by a constant. Therefore, the computationally efficient MP2 method was used to determine the basis set to be used. Figure 2 shows that the energy almost converges at the 6-31+g(3d) and 6-31+g(3df) basis sets. While the 6-31+g(3df) basis set gives only a slightly more attractive energy than the 6-31+g(3d) basis set, the computational time required is significantly longer. As a result of the compromise between accuracy and computational time, the 6-31+g(3d) basis set was used as the largest basis set. Even using the two smaller segments from cut_1, to compute the interactions with CO_2 using the CCSD(T)/6-31+g(3d) is still computationally intensive. Therefore, the Hybrid Method for Interaction Energies (HM-IE)[27] recently developed by us has been used here. This method can be used to accurately approximate the interaction energies from a high level method plus a large basis set while requiring considerably less computational time and resources and has been tested for a variety of systems. The details of HM-IE can be found elsewhere.[27] In this study, a large basis set 6-31+g(3d), a medium basis set 6-31g(d), and a small basis set 3-21(g) were used in applying the two-step HM-IE (MP2-4:CC).

The interaction energies of CO_2 with the two segments from cut_1 were computed with the HM-IE using the Gaussian 98 suite of programs.[28] The basis set superposition errors in all computations were compensated for by using the counterpoise correction method.[29] Different CO_2 separation distances and orientations (14) were selected in both the attractive and repulsive interaction regions. The total CPU time was about 350 days on a single AMD MP 1800+ processor. In the QM computations, all sources of interactions between CO_2 and the carbon surface, including electrostatic interactions, have been included. For ease of use in molecular simulation, these interaction energies were then fitted to the pairwise additive site−site LJ potential given by eq 1, though other types of potentials could have been used. Note that the LJ potential had also been used to fit measured gas adsorption properties at zero coverage on planar graphite in developing the Steele potential. The difference between our ab initio and the Steele potentials is solely in the parameters. In other words, we determine how the potential parameters are affected by the topology of the carbon surface and then how the potential parameters alter the adsorption behavior. Figure 3 shows the interaction energies computed from QM compared to those from the fitted LJ potential. The fit is satisfactory with the average absolute deviation of only 0.545 kJ/mol. The four adjustable LJ potential parameters for the CO_2-C_{168} interaction from the fit are given in Table 1, along with the parameters for

(27) Klauda, J. B.; Garrison, S. L.; Jiang, J. W.; Arora, G.; Sandler, S. I. *J. Phys. Chem. A* **2004**, *108*, 107.

(28) Frisch, M. J.; Trucks, G. W.; Schlegel, H. B. et al. *Gaussian 98*, revision A.11.3 ed.; Gaussian, Inc.: Pittsburgh, PA, 2002.

(29) Boys, S. F.; Bernardi, F. *Mol. Phys.* **1970**, *19*, 553.

N_2-C_{168} interaction from our previous work.[17] For comparison, the LJ parameters of the empirical Steele potential for N_2[13,14] and CO_2[30] interactions with planar graphite are also listed. As a consequence of the nonzero surface curvature and nonaromatic ring structure in the C_{168} structure, the parameters in the ab initio potential obtained by us are different from those in the Steele potential. Compared to the Steele potential, the well depths in the ab initio potential are larger for both N_2 and CO_2, and the collision diameters $\sigma_{\underline{C}-N}$ and $\sigma_{\underline{C}-CO_2}$ in the ab initio potential are also larger, but $\sigma_{\underline{C}-CO_2}$ is slightly smaller. As we shall see, the adsorption predicted with the ab initio potential is higher than that with the Steele potential.

III. Simulation Method

Grand canonical Monte Carlo (GCMC) simulations[31,32] at fixed adsorbate chemical potential μ, volume V, and temperature T were carried out for the adsorption of pure CO_2 and N_2 and their mixture in the C_{168} schwarzite. Because the chemical potentials of adsorbate in the adsorbed and bulk phases are identical at thermodynamic equilibrium, GCMC simulation allows one to directly relate the chemical potentials of the adsorbate in both phases and has been used widely for the simulation of adsorption.[33]

In this work we consider gas adsorption at low and moderate pressures at room temperature $T = 300$ K, as a consequence we assume that the bulk pure gas and gas mixture are ideal gases. Nevertheless, at high pressures the nonideality of the gas phase should be taken into account, e.g., by an equation of state or by simulation at a fixed bulk pressure.[12,34] The simulation box representing the NPC adsorbent contained 8 ($2 \times 2 \times 2$) C_{168} schwarzite unit cells with periodic boundary conditions in all three dimensions. A test using a larger simulation box of 27 ($3 \times 3 \times 3$) unit cells did not, within statistical error, give discernibly different results. A spherical cutoff length of 21.8 Å, half the simulation box length, was used in the evaluation of the LJ intermolecular interaction with the long-range correction added. For the Coulombic interaction, a simple spherical truncation could result in significant errors,[35] and the Ewald sum with a tin-foil boundary condition (a surrounding dielectric constant of infinity) was used instead.[36] The real/reciprocal space partition parameter and the cutoff for reciprocal lattice vectors were chosen to be 0.2 and 8, respectively, to ensure the convergence of the Ewald sum.

The number of trial moves in a typical simulation was 2×10^7, though additional trial moves were used at high coverages. The first 10^7 moves were used for equilibration, and the second 10^7 moves to obtain ensemble averages. For the adsorption of a pure gas, five types of trial moves were randomly attempted in the GCMC simulation, namely, translation, rotation, and partial regrowth at a neighboring position; complete regrowth at a new position; and exchange with the reservoir including creation and deletion with equal probability. For the adsorption from a mixture, in addition, exchange of molecular identity was used, i.e., CO_2 to N_2 and vice versa, with equal probability. While this trial move is not required in the GCMC simulation, its use allows reaching equilibrium faster and reduces fluctuations after equilibration.[37]

In adsorption process, the isosteric heat rather than the adsorption isotherm is often used to ascertain the adsorption mechanism, as the isosteric heat is more sensitive to the change of adsorption energy. The isosteric heat was calculated from

$$q_{st} = RT - \left[\frac{\partial(U_{a,total} - U_{b,intra})}{\partial N_a}\right]_{T,V} \quad (3)$$

where R is gas constant; N_a is the molar number of adsorbed molecules; $U_{a,total}$ is the total adsorption energy, including contributions from both adsorbate−adsorbent and adsorbate−adsorbate interactions; and $U_{b,intra}$ is the total intramolecular energy of the adsorbate in bulk phase. Consequently, $(U_{a,total} - U_{b,intra})$ accounts for the difference in the intramolecular energies of the adsorbate between adsorbed and bulk phases. In our previous studies of the adsorption of N_2 and O_2 on various carbon-based materials,[11,12,18,19,34,38] the adsorbate was modeled as a rigid diatomic molecule, and therefore the value of $U_{b,intra}$ was equal to zero, which is not the case here for CO_2.

In the limit of zero coverage, the affinity between adsorbate and adsorbent is usually described by the zero-coverage isosteric heat of adsorption and the Henry constant, which here were calculated from a canonical Monte Carlo (NVT) simulation with a single gas molecule to represent zero coverage. In the NVT simulation, four types of trial moves were randomly performed, including translation, rotation, partial regrowth, and complete regrowth. In this approach, the limiting isosteric heat of adsorption q_{st}^0 was calculated from

$$q_{st}^0 = RT - (\langle U_{a,total}^0 \rangle - \langle U_{b,intra}^0 \rangle) \quad (4)$$

where $\langle U_{a,total}^0 \rangle$ is the ensemble averaged total adsorption energy of a single gas molecule in an empty adsorbent, and $\langle U_{b,intra}^0 \rangle$ is that of a single gas molecule in the ideal-gas state and is due to the intramolecular interaction. These were evaluated from

$$\langle U_{a,total}^0 \rangle = N_A \frac{\int u_a(\mathbf{r},\varpi) \exp[-\beta u_a(\mathbf{r},\varpi)] d\mathbf{r} d\varpi}{\int \exp[-\beta u_a(\mathbf{r},\varpi)] d\mathbf{r} d\varpi} \quad (5)$$

$$\langle U_{b,intra}^0 \rangle = N_A \frac{\int u_{intra}(\mathbf{r},\varpi) \exp[-\beta u_{intra}(\mathbf{r},\varpi)] d\mathbf{r} d\varpi}{\int \exp[-\beta u_{intra}(\mathbf{r},\varpi)] d\mathbf{r} d\varpi} \quad (6)$$

where N_A is the Avogadro number, $\beta = 1/k_B T$ and k_B is the Boltzmann constant, $\mathbf{r}$ is the position vector, and ϖ is the orientation vector of the gas molecule.

The Henry constant K_H was calculated from

$$K_H = \frac{N_A}{RT\rho} \frac{\exp(-\beta \mu_{ex,a}{}^0)}{\exp(-\beta \mu_{ex,b}{}^0)} = \frac{N_A}{RT\rho_{\underline{C}}} \frac{\int \exp[-\beta u_a(\mathbf{r},\varpi)] d\mathbf{r} d\varpi}{\int \exp[-\beta u_{intra}(\mathbf{r},\varpi)] d\mathbf{r} d\varpi} \quad (7)$$

where $\rho_{\underline{C}} = 1.294$ g/cm^3 is the density of the C_{168} schwarzite framework, $\mu_{ex,a}^0$ and $\mu_{ex,b}^0$ are the excess chemical potentials of a single gas molecule in an empty adsorbent and of the single gas molecule itself in bulk phase, respectively. From the complete regrowth move, which is equivalent to the Widom test-particle insertion method,[39] the excess chemical potential was evaluated.

IV. Results and Discussion

Table 2 gives the limiting isosteric heats q_{st}^0 and Henry constants K_H for pure N_2 and CO_2, respectively, adsorption in the C_{168} schwarzite. As CO_2 has one more interaction site than N_2 and interacts with surface more strongly, with both the Steele and ab initio potentials, the values of q_{st}^0 and K_H for CO_2

(30) Bottani, E. J.; Ismail, I. M. K.; Bojan, M. J.; Steele, W. A. *Langmuir* **1994**, *10*, 3805.
(31) Allen, M. P.; Tildesley, D. J. *Computer simulation of liquids*; Clarendon Press: Oxford, 1987.
(32) Frenkel, D.; Smit, B. *Understanding Molecular Simulations: From algorithms to applications*, 2nd ed.; Academic Press: San Diego, 2002.
(33) Nicholson, D.; Parasonage, N. G. *Computer Simulation and the Statistical Mechanics of Adsorption*; Academic Press: New York, 1982.
(34) Jiang, J. W.; Sandler, S. I. *Phys. Rev. B* **2003**, *68*, 245412.
(35) Fuller, N. G.; Rowley, R. L. *Int. J. Thermophys.* **1998**, *19*, 1040.
(36) Heyes, D. M. *Phys. Rev. B* **1994**, *49*, 755.
(37) Kofke, D. *Mol. Simul.* **1991**, *7*, 285.
(38) Jiang, J. W.; Wagner, N. J.; Sandler, S. I. *Phys. Chem. Chem. Phys.* **2004**, *6*, 4440.
(39) Widom, B. *J. Chem. Phys.* **1963**, *39*, 2802.

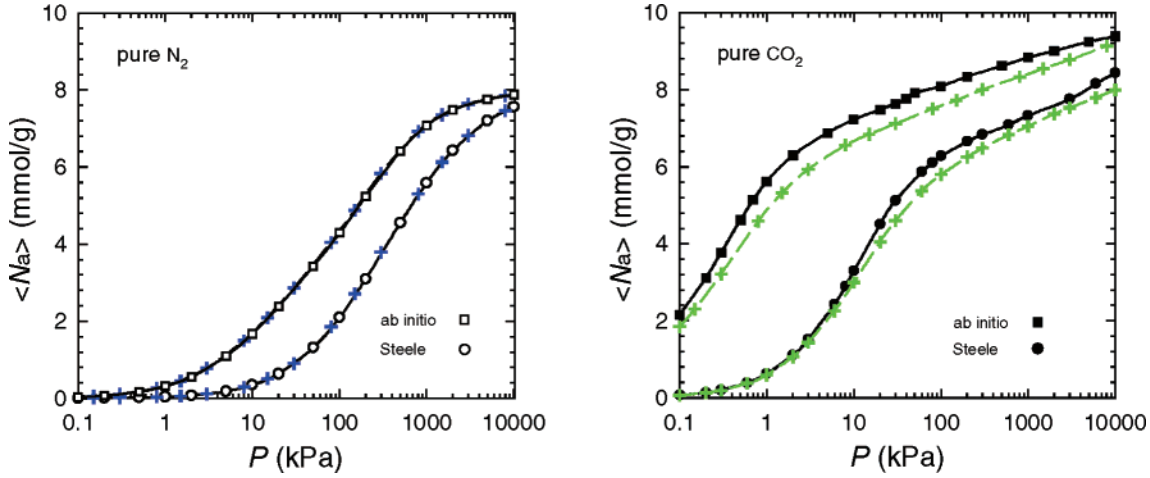

Figure 4. Adsorption isotherms of pure N_2 and CO_2, respectively, in the C_{168} schwarzite. The unfilled circles (N_2) and filled circles (CO_2) are from the Steele potential; the unfilled squares (N_2) and filled squares (CO_2) are from the ab initio potential. The crosses are additional simulation results neglecting the adsorbate quadrupole moment.

Table 2. Limiting Isosteric Heats q_{st}^0 and Henry Constants K_H of Pure N_2 and CO_2 Adsorption in the C_{168} Schwarzite

	ab initio potential		Steele potential	
	N_2	CO_2	N_2	CO_2
q_{st}^0 (kJ/mol)	28.85	43.36	21.98	32.45
K_H (mol/kg/kPa)	0.34	34.42	0.038	0.68

adsorption are significantly higher than those for N_2 adsorption. Compared to the Steele potential, the ab initio potential is more attractive and results in larger values of q_{st}^0 and K_H for both N_2 and CO_2. As given in Table 1, the collision diameter σ_{C-N} and well depth ϵ_{C-N} in the ab initio potential are larger than those in the Steele potential; either of the two factors separately leads to a stronger attraction for N_2 with the carbon surface.[11,18] Likewise, the ab initio potential results in a stronger CO_2-C_{168} attraction than the Steele potential.

Figure 4 shows the adsorption isotherms of pure N_2 and CO_2, respectively, in the C_{168} schwarzite predicted with the ab initio and Steele potentials. Over the pressure range under study, the isotherms are of type I (Langmuirian), which is the characteristic of a microporous adsorbent with pores of molecular dimensions (below 2 nm).[40] For each species, the ab initio potential results in a larger extent of adsorption than the Steele potential, especially for CO_2 at low pressures. The extent of adsorption of CO_2 is larger than that of N_2 as the interaction of CO_2 with the surface is stronger, an energetic effect. Note that the adsorption of both CO_2 and N_2 are not saturated at 10 000 kPa and will increase with increasing pressure until saturation. At still higher pressures, the extent of N_2 adsorption becomes larger than that of CO_2. This is due to an entropic effect in that N_2 has a smaller molecular size and can fit into the partially filled pores more easily. Similar behavior was observed in our previous study of the adsorption of pure O_2 and N_2 in the C_{168} schwarzite.[11,18] In addition, we considered adsorption neglecting the adsorbate quadrupole moment, that is, with the partial charges of the adsorbate molecule turned off; the results are shown by the crosses in Figure 4. The neglect of Q_{N_2} does not give discernibly different results of N_2 adsorption from those obtained by including Q_{N_2}, similar to the reported N_2 adsorption

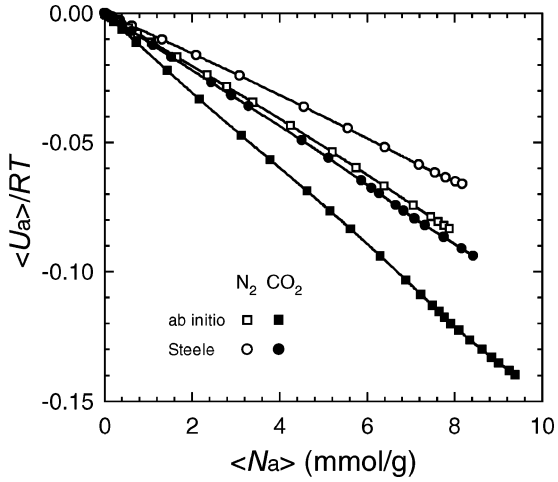

Figure 5. Adsorption energies of pure N_2 and CO_2, respectively, in the C_{168} schwarzite as a function of coverage.

in slit-shaped micropores.[41] However, a lesser extent of CO_2 adsorption is found when Q_{CO_2} is set to zero except at low coverages. This suggests that, as Q_{CO_2} is three times larger than Q_{N_2}, the incorporation of Q_{CO_2} is important, particularly, at high coverages.

Figure 5 shows the adsorption energies of pure CO_2 and N_2, respectively, in the C_{168} schwarzite as a function of coverage. There are two contributions to the adsorption energy, one from the adsorbate−adsorbate interaction and the other from the adsorbate−adsorbent interaction. As the extent of adsorption, the adsorption energy of CO_2 is greater than that of N_2, and the ab initio potential leads to a more attractive adsorption energy than the Steele potential. The adsorption energies are almost linear with coverage over the pressure range studied, and such a simple relation gives us only limited information about adsorption. However, as we shall see below, the isosteric heat of adsorption provides more detailed adsorption information.

Figure 6 shows the isosteric heats of adsorption of pure CO_2 and N_2, respectively, as a function of coverage. Extrapolated to zero coverage, q_{st} values here are approximately equal to q_{st}^0 values given in Table 2, which were calculated from the NVT

(40) Rouquerol, F.; Rouquerol, J.; Sing, K. *Adsorption: By Powders and Porous Solids*; Academic Press: London, 1999.

(41) Kaneko, K.; Cracknell, R. F.; Nicholson, D. *Langmuir* **1994**, *10*, 4606.

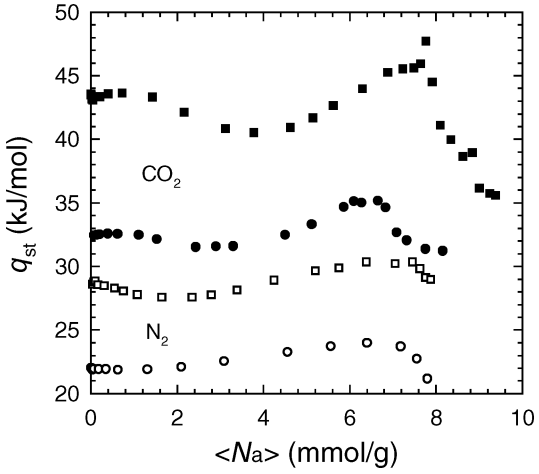

Figure 6. Isosteric heats of pure N_2 and CO_2 adsorption, respectively, in the C_{168} schwarzite as a function of coverage.

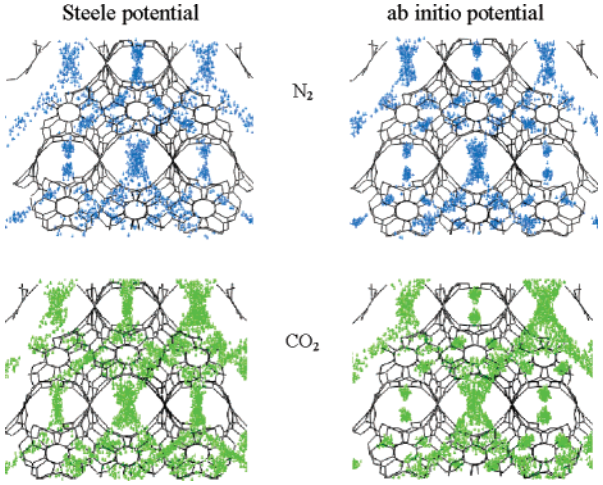

Figure 7. Center-of-mass density distributions of pure N_2 (blue) and CO_2 (green) adsorption in the C_{168} schwarzite at 1000 kPa. Views are on the (110) plane. Left with the Steele potential, right with the ab initio potential.

simulations. Similar to the adsorption isotherm and adsorption energy, q_{st} of CO_2 is larger than that of N_2 with both potentials; and the ab initio potential results in larger values of q_{st} for both CO_2 and N_2. The isosteric heat of adsorption is related to the derivative of adsorption energy with respect to coverage, is more sensitive as a function of coverage than the adsorption energy, and can be used to deduce information on the adsorption process.

There are two types of isosteric heat behavior shown in Figure 6. With increasing coverage, the q_{st} of N_2 calculated with the Steele potential increases slowly to a maximum and then decreases rapidly. Such behavior has been observed experimentally, for example, in the adsorption of Xe in zeolites X and Y,[42] of Ar in $AlPO_4$-5,[43] and of CH_4 in a fcc-structured silica gel.[44] The increase of q_{st} is largely because of the cooperative adsorbate−adsorbate attractions. The later decrease of q_{st} results from two factors, additional admolecules have to occupy an energetically less favorable adsorption region leading to a weaker adsorbate−adsorbent attraction and also a weaker adsorbate−adsorbate attraction due to the shorter separation distance between the admolecules in the limited available space.

The isosteric heat of N_2 calculated with the ab initio potential and that of CO_2 calculated with both potentials show a different behavior. With increasing coverage, q_{st} first decreases to a minimum, then increases to a maximum, and finally decreases. The stronger the gas−surface interaction potential is, the more evident is the initial decrease, and the higher are the coverages at which the minimum and maximum occur. This type of behavior is not unusual and has been observed in experimental studies, such as, the adsorption of N_2 and CO in $AlPO_4$-5,[43] of CH_4 in a silica gel with a hard sphere structure,[44] of Ar in chabazite,[45] and of CH_4 in activated carbon.[46] The initial decrease of q_{st} is a consequence of the heterogeneous character of the C_{168} schwarzite surface, in which the more energetically favorable sites for adsorption are occupied first, and then the less favorable sites are occupied as the coverage increases. Note that there is no apparent initial decrease of q_{st} for N_2 adsorption with the Steele potential. This does not mean that the C_{168} schwarzite surface is homogeneous in this case; instead, it is because the N_2−C_{168} Steele potential is not strong enough to reflect the surface heterogeneity. The later increase of q_{st} is due to the cooperative adsorbate−adsorbate attraction; and finally, the decrease of q_{st} results from the weaker adsorbate−adsorbent and adsorbate−adsorbate attractions at increased coverages.

Figure 7 shows the density distributions of the centers-of-mass of adsorbed pure CO_2 and N_2, respectively, at 1000 kPa generated by accumulating 50 equilibrium configurations. The linked black network is the C_{168} schwarzite unit cell structure, and the blue and green points are the centers-of-mass of the adsorbed N_2 and CO_2 molecules, respectively. The centers-of-mass are not distributed uniformly, and there is a preference for alignment along the channel intersections and localization in the small pores. With the ab initio potential, as the adsorption is greater, the localization in the small pores is more pronounced for both N_2 and CO_2. In our previous study,[11] we have found that, on going from low to high pressure with gradually increasing number of admolecules, the center-of-mass density distribution shows an interesting shift. At low pressures, the density distribution is nonuniform but continuous in both types of pores. However, the distribution in the small pores becomes localized at modest pressures, and in particular, there are no admolecules at the center of the small pores. Finally, at high pressures, the center-of-mass distribution in the large pores also becomes more localized. The occurrence of the localization is due to the competitive balance between energetic and entropic effects. With increasing pressure, the adsorbate−adsorbate attraction first increases at low pressures but then decreases at modest pressures because as the number of admolecules increases the separation distance between the admolecules becomes shorter, particularly, in the small pores, which leads to a more localized density distribution in the small pores. A further increase in pressure results in a further decrease in the adsorbate−adsorbate separation distance and a decrease in attraction (and perhaps even a repulsion), and the same

(42) Woods, G. B.; Rowlinson, J. S. *J. Chem. Soc., Faraday Trans. 2* **1989**, *85*, 765.
(43) Grillet, Y.; Llewellyn, P. L.; Tosi-Pellenq, N.; Rouquerol, J. "Adsorption of Argon, Methane, Nitrogen, Carbon Monoxide and Water Vapour on Sepiolite and AlPO4−5 as Studied by Isothermal Microcalorimetry"; Fundamentals of adsorption: proceedings of the Fourth International Conference on Fundamentals of Adsorption, 1992, Kyoto, Japan.
(44) Vuong, T.; Monson, P. A. *Langmuir* **1996**, *12*, 5425.
(45) Rudzinski, W. Fundamentals of Single-Gas and Mixed-Gas Adsorption on Heterogeneous Solid Surfaces. In *Physical Adsorption: Experiment, Theory and Applications*; Fraissard, J., Ed.; Kluwer Academic Publishers: Dordrecht, The Netherlands, 1997; p 181.
(46) Choi, B. K.; Choi, D. K.; Lee, Y. W.; Lee, B. K.; Kim, S. H. *J. Chem. Eng. Data* **2003**, *48*, 603.

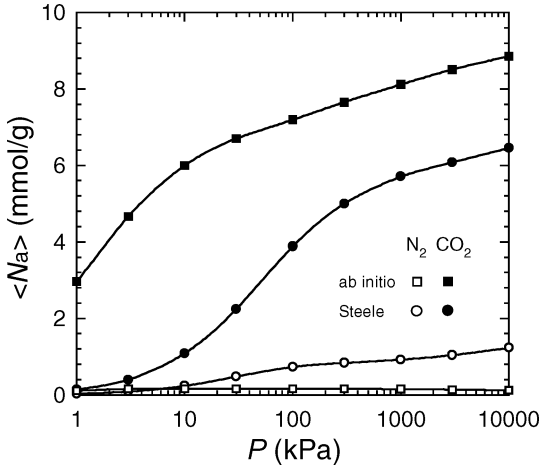

Figure 8. Adsorption isotherm of CO_2-N_2 mixture (bulk composition $CO_2/N_2 = 0.21:0.79$) in the C_{168} schwarzite as a function of the total bulk pressure.

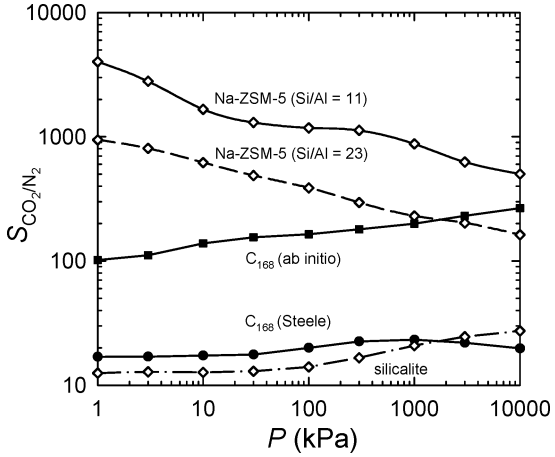

Figure 9. Selectivity of CO_2 over N_2 as a function of the total bulk pressure (bulk composition $CO_2/N_2 = 0.21:0.79$) in the C_{168} schwarzite (with the Steele and ab initio potentials), silicalite, Na−ZSM-5 (Si/Al = 23), and Na−ZSM-5 (Si/Al = 11).

phenomenon that has occurred in the small pores then occurs in the large pores.

We next consider the competitive adsorption of CO_2 and N_2 in flue gases. There may exist many components in a flue gas; however, a model flue gas is studied here only consisting of CO_2 and N_2. The bulk molar ratio of CO_2 to N_2 in the model flue gas is 0.21:0.79, which corresponds to the flue gas emitted from the complete combustion of carbon with air. Figure 8 shows the adsorption isotherm of the model flue gas as a function of total bulk pressure in the C_{168} schwarzite. Because CO_2 interacts energetically more strongly than N_2 with the surface, CO_2 is preferentially adsorbed. Even though the bulk partial pressure of N_2 is almost 4 times that of CO_2, the amount of N_2 adsorption is much less than that of CO_2, especially when simulated with the ab initio potential. The amounts of both CO_2 and N_2 increase with increasing pressure over the whole range of pressure studied. However, it can be expected that, with further increases in pressure, the size effect will become dominant and the amount of adsorbed N_2 will continue to increase while the amount of adsorbed CO_2 will decrease. Finally, the pores will be completely filled, and the adsorption of both gases will reach saturation. Compared with the results using the Steele potential, the ab initio potential results in a larger difference between the amounts of adsorbed CO_2 and N_2, and as we shall see, the selectivity between the two gases from the model flue gas is greater.

Adsorption selectivity is a key parameter describing the competitive adsorption between two components. Here the selectivity of CO_2 over N_2 is defined as $S_{CO_2/N_2} = (x_{CO_2}/y_{CO_2})/(x_{N_2}/y_{N_2})$, where x and y are the compositions in the adsorbed and bulk phases, respectively. Figure 9 shows S_{CO_2/N_2} from the model flue gas as a function of the total bulk pressure. With the Steele potential, the value of S_{CO_2/N_2} in the C_{168} schwarzite first increases slightly and then decreases with increasing pressure, and the overall value is approximately 20. With the ab initio potential, the S_{CO_2/N_2} increases with increasing pressure, with values between 100 and 300 over the pressure range of this study. Although not shown, S_{CO_2/N_2} with either potential is expected to become a constant when saturation is approached. The large value of S_{CO_2/N_2}, particularly as predicted with the ab initio potential, implies that the separation factor between CO_2 and N_2 by selective adsorption from the model flue gas is quite large.

As mentioned in section 1, zeolite membranes have been used to separate CO_2 and N_2 by competitive adsorption.[7] For comparison, the adsorption of pure CO_2 and N_2 and their mixture were simulated here in ZSM-5 zeolites, which are the most frequently studied prototype zeolite. The model, potential, simulation method, and results are given in the Supporting Information. As shown in Table S2 and Figure S1, the simulated limiting isosteric heats of CO_2 and N_2 and the adsorption isotherm of CO_2 in silicalite are in accord with experimentally measured data, implying the accuracy of the adsorbate−silicalite interaction potentials. Figure 9 also shows the simulated selectivity S_{CO_2/N_2} for the adsorption of the model flue gas in all-silica (silicalite) and two types of Na-exchanged ZSM-5 (Na−ZSM-5) zeolites. The presence of the nonframework Na^+ has significant impact on the adsorption and selectivity. With decreasing Si/Al ratio and hence increased number of Na^+ in the ZSM-5 zeolite, CO_2 adsorption increases while N_2 adsorption decreases, which leads to a greater selectivity of CO_2 over N_2. This is because CO_2 has a large quadrupole moment and its adsorption is remarkably enhanced due to the electric field of Na^+. Compared to S_{CO_2/N_2} in the C_{168} schwarzite predicted with either the ab initio or the Steele potential, S_{CO_2/N_2} is generally smaller in silicalite but greater in Na−ZSM-5 zeolites.

V. Conclusions

The adsorption of pure CO_2 and N_2 and their mixture in the C_{168} schwarzite as an adsorbent model for nanoporous carbons has been studied using a multiscale approach. From first-principle quantum mechanics, the ab initio adsorbate−adsorbent potential has been developed. Having taken into account the rehybridization of carbon atoms and the localization of electron densities, which are caused by the nonzero curvature and nonaromatic ring structure of the C_{168} schwarzite surface, the ab initio potential is expected to be more accurate for use with curved nanoporous carbons than the commonly used empirical Steele potential which is based on gas adsorption on planar graphite. The ab initio and Steele potentials have been both used in full atomistic molecular simulations to predict adsorption

behavior. With the ab initio potential, greater adsorption for both CO_2 and N_2, and a larger separation factor between the two gases in their binary mixture are found than with the Steele potential. The results demonstrate the sensitivity of the predicted adsorption behavior to the interaction potential used. This work reveals that the empirical Steele potential may not lead to accurate prediction for adsorption on a carbon-based material with a curvature and ring structure that are very different from planar graphite. Finally, our results based on the ab initio potential suggest that nanoporous carbon adsorbents, such as the C_{168} schwarzite, can be useful for the separation of flue gases, and the efficacy is between that of all-silica and Na-exchanged ZSM-5 zeolites.

Acknowledgment. We gratefully acknowledge the financial support from Grant No. DE-FG02-85ER13436 of the Department of Energy and Grants No. CTS-0083709 and EEC-0085461 of the National Science Foundation. We thank Dr. Jeffery B. Klauda for helpful discussions.

Supporting Information Available: The adsorption of pure CO_2 and N_2 and their mixture in all-silica and Na-exchanged ZSM-5 zeolites from Monte Carlo simulation. This material is available free of charge via the Internet at http://pubs.acs.org.

JA0424575